X-621-68-383
PREPRINT

NASA TM X-63382

ELECTRON MEASUREMENTS BEARING ON THE ENERGY AND PARTICLE BALANCE OF THE UPPER F-REGION

L. H. BRACE,
H. G. MAYR,
J. A. FINDLAY

SEPTEMBER 1968

GSFC
GODDARD SPACE FLIGHT CENTER
GREENBELT, MARYLAND

X-621-68-383

PREPRINT

ELECTRON MEASUREMENTS BEARING ON THE ENERGY AND PARTICLE BALANCE OF THE UPPER F-REGION

L. H. Bruce, H. G. Mayr, and J. A. Findlay

September 1968

GODDARD SPACE FLIGHT CENTER

Greenbelt, Maryland

ELECTRON MEASUREMENTS BEARING ON THE ENERGY AND PARTICLE BALANCE OF THE UPPER F-REGION

L. H. Brace, H. G. Mayr, and J. A. Findlay

ABSTRACT

Electron temperature and density profiles measured between 120 and 630 kilometers at midday at Wallops Island on March 2, 1966 are presented and interpreted. The temperature profile exhibits a strong positive gradient (24°/km) below 150 kilometers followed by a smooth transition to a much smaller positive gradient (1.5°/km) above 300 kilometers. Between 300 and 400 kilometers, the electron density decreases with a scale height of about 100 kilometers, which is significantly lower than the diffusive equilibrium scale height for the observed temperatures. Furthermore, the scale height more than doubles between 400 and 500 kilometers. This change in scale height in a region where the mean ion mass and the electron temperature are nearly constant is also inconsistent with diffusive equilibrium and suggests that some dynamic process was occurring at the time of the flight.

A simultaneous solution of the particle and energy continuity equations for the F-region is carried out with the aid of inputs and boundary conditions from measurements of neutral composition, neutral gas temperature, and ion composition from the same vehicle. This analysis permits us to conclude that the upper F-region was not in diffusive equilibrium between 300 and 500 kilometers and that the low plasma scale height at these altitudes was consistent with either a neutral atmospheric wind or a rapid temporal variation in O^+.

CONTENTS

ELECTRON MEASUREMENTS BEARING ON THE ENERGY AND PARTICLE BALANCE OF THE UPPER F-REGION

INTRODUCTION

On March 2, 1966 at 17:59:42 UT a Javelin rocket (NASA 8.25) carried a multiple experiment package into the atmosphere above Wallops Island, Virginia. The payload, shown in Figure 1, included a magnetic type neutral mass spectrometer (Cooley and Reber, 1968), two Bayard-Alpert-type neutral density gauges (Pelz and Newton, 1968), a Bennett type ion mass spectrometer (Brinton, et al., 1968), two retarding potential analyzers, a c-w propagation experiment, and a cylindrical electrostatic probe. From these instruments it has been possible to derive altitude profiles of the ion and neutral composition as well as the electron and ion concentrations and temperatures.

The purpose of this paper is to present the cylindrical probe measurements of electron temperature (T_e) and density (N_e) and to employ those results to examine the particle and energy balance of the topside of the ionosphere on that occasion. The ion composition measurements are drawn upon for certain boundary conditions in the calculations.

THE EXPERIMENT

The theory and implementation of the cylindrical electrostatic probe measurement have been discussed in detail elsewhere (Spencer, Brace, Carignan, Taeusch, Nieman, 1965) (Brace and Reddy, 1965) (Brace, Reddy and Mayr, 1967) but will be reviewed briefly here.

As shown in Figure 1, the probe sensor is mounted on the side of the instrument housing and protrudes outward about 18 inches into the plasma which surrounds the payload when in flight. The initial 9 inches of the sensor is insulated from the collector and acts as a guard electrode. The collector itself is 9 inches long and 0.022 inches in diameter and, like the guard, is made of stainless steel.

The potential of both the guard and collector are swept linearly from -1.1 volts to +2.4 volts at the rate of 6 sweeps per second. A +5 volt step is applied for about 15 milliseconds before and after each sweep to provide additional spatial resolution in the electron saturation current used to derive N_e.

Because of the high spin rate (1 rps), employed to maintain attitude stability of the payload, it was necessary to use the shortest sweep period consistent with amplifier and telemetry frequency response. The 160 millisecond period employed permitted each volt-ampere curve to be resolved while the probe rotated through an angle of less than 50°, thus minimizing distortion of the curves due to the spinning motion. The high sweep rate produced a much greater spatial resolution than was needed throughout most of the flight. Therefore curves were selected to provide approximately uniform height resolution except where indications of structure were present. Curves recorded while the probe rotated through the wake of the vehicle were rejected, although this was not a consideration during most of the ascent when the vehicle spin axis was aligned more or less with the velocity vector.

Figure 2 shows sequences of typical volt-ampere characteristics recorded at selected altitudes on upleg and downleg. The current detector range was continuously stepped through the sequence shown.

The Electron Density

The electron density is derived from cur 'es such as shown in Figure 2 by employing the Langmuir probe equations for an orbital limited cylinder; that is, a collector having a radius much smaller than the plasma Debye length. The electron saturation current in this case is given by

$$I_e = A N_e e \left(kT_e / 2\pi\, m_e\right)^{1/2} 2/\pi^{1/2} \left(1 + eV/kT_e\right)^{1/2} \qquad (1)$$

where

I_e = electron current

m_e = electron mass

e = electron charge

V = potential of probe relative to plasma

k = Boltzmann constant

A = area of probe collector.

Spencer et al. (1965) pointed out that the electron saturation curve (1) becomes independent of T_e for large potentials ($eV/kT >> 1$), and the saturation current reduces to

$$I_e = A N_e e/\pi \left(2\, eV/m_e\right)^{1/2}, \qquad (2)$$

This fact permits a simplification in the analysis of large amounts of data because the electron current amplitude depends only upon N_e and the potential V, which can be determined readily from the curves themselves. Therefore an altitude profile of electron current is related to an N_e profile by a constant.

The Electron Temperature

The electron temperature is derived from the retarding potential region of the characteristic described by

$$I_e = A N_e e (kT_e/2\pi m_e)^{1/2} \exp(eV/kT_e) \qquad (3)$$

which reduces to

$$T_e = e/k \left(dV/d \ln I_e\right) = 1.16 \times 10^4 \left(dV/d \ln I_e\right) . \qquad (4)$$

In practice, I_e is measured at several voltages within the retarding region of each curve, and the derivative in (4) is determined curve by curve throughout the flight.

THE MEASUREMENTS

Owing to the forward ejection of the protective nose cone, the volt-ampere curves recorded during the initial 20 seconds after ejection were distorted and badly depressed in amplitude. The currents also exhibited extreme fine structure, as the bottom sequence in Figure 2 demonstrates. The ablation of material from the nose cone, designed to present excessive heating, is probably

responsible for the great extent of the wake and its highly structured nature. Above 250 kilometers, the current characteristics assumed their usual smooth nature and remained smooth throughout the flight, also evident in Figure 2.

Electron Density

The electron saturation currents measured at the +5 volt steps are shown in Figure 3 for upleg and Figure 4 for downleg. Clearly, in the region below 260 kilometers, the payload was in the deep wake of the nose cone. It appears that some residual nose cone wake effect extends up to about 310 kilometers on upleg as will be demonstrated.

Vehicle wake effects are also evident in Figures 3 and 4. The upleg currents exhibit much smaller scatter than the downleg currents because the probe did not pass through the full wake of the vehicle on upleg. On downleg, however, the spin axis was nearly perpendicular to the trajectory and the wake currents were as much as a factor of ten below the nonwake currents at the lowest altitudes where the velocity was highest. The points below the dashed line on Figure 4 were rejected on this basis. The source of the remaining scatter has not been firmly identified, but it is probably related to additional orientation effects such as the variation of the angle between the probe and the magnetic field or the velocity vector.

The N_e points shown in Figure 5 were derived by averaging all the current values within each 10 kilometer altitude interval and applying Equation 2. The solid points show the upleg values and the crosses show the downleg values.

The circled points were derived from the ionosonde record taken simultaneously at Wallops Station (private communication J. Jackson). Since we cannot uniquely identify the upper boundary of the nose cone wake effects seen on upleg, we have arbitrarily interpolated between the ionosonde data at the F_2 maximum (250 kilometers) and the probe data above 320 kilometers. The solid lines represent a free-hand fit to the points above 320 kilometers on upleg and to all the downleg points.

Electron Temperature

The electron temperature analysis began to yield consistent results soon after nose cone ejection, even where the magnitude of the currents was depressed by more than a factor of 10 in the nose cone wake. Groups of about 5 volt-ampere curves were selected at approximately 20-kilometer intervals and the mean value of each group is shown in Figure 6. The horizontal bars represent the standard deviation of each set. The telemetry signal was lost at 110 kilometers on downleg where the rocket passed below the local horizon at Wallops Station.

Horizontal Gradient

As a result of the horizontal motion of the rocket (approx. 1 km/sec) as it traveled eastward over the Atlantic ocean, the data taken near apogee may contain significant horizontal structure. This probably accounts for the 30% difference in the electron density on upleg and downleg. The T_e data do not show

this effect as strongly. In either case, however, caution should be used in employing the data above about 500 kilometers without a suitable correction for the observed horizontal gradients.

DISCUSSION

An examination of the N_e profiles between 300 and 400 kilometers reveals that the scale height is only about half that which would be expected in diffusive equilibrium at the observed temperature (assuming $T_i = T_e$). Furthermore a factor of two increase in the scale height occurs between 400 and 500 kilometers where no corresponding change in the temperature and composition is observed (Brinton, et al., 1968). The scale height at higher altitudes, although somewhat obscured by the horizontal gradient, is reasonably consistent with diffusive equilibrium as will be noted later.

In the following analysis we attempt to account for the reduced scale height below 400 kilometers by introducing (1) an ion-neutral drag which produces a downward force on the O^+ population, or (2) a temporal variation in the O^+ distribution which produces an upward flux of O^+ and a resultant ion-neutral drag in the downward direction. Either of these dynamic effects, or a combination, can reproduce the observed scale heights; however, Brinton et al., (1968) have employed the ion composition measurements taken on this flight to argue against the upward O^+ ion flux.

The Particle Equations

In the following analysis we consider only the ions O^+ and H^+, by far the major ions observed in the upper F region on this flight (Brinton et al., 1968). We assume that O^+ is produced by photoionization of O and is lost by charge transfer to N_2. We assume that the source and sink for H^+ is the charge exchange reaction

$$O^+ + H \rightleftharpoons H^+ + O \; . \tag{5}$$

Since this reaction involves O^+, it is also included in the O^+ continuity equation. We further consider only field-aligned transport processes.

The resulting continuity equations for O^+ and H^+ have the form

$$\frac{\partial [O^+]}{\partial t} = p[O] - L[O^+]\,[N_2] - 9/8\,K[O^+]\,[H] + K[O]\,[H^+] - B\,\partial/\partial s\left([O^+]\,v_{O^+}/B\right) \tag{6}$$

and

$$\frac{\partial [H^+]}{\partial t} = 9/8\,K[O^+]\,[H] - K[O]\,[H^+] - B\,\partial/\partial s\left([H^+]\,v_{H^+}/B\right) \tag{7}$$

where

p = photoionization rate coefficient

L = recombination rate coefficient

K = charge exchange rate coefficient

s = distance along the field line

B = magnetic field intensity

v = ion transport velocity parallel to field.

Assuming no charge transport across the equator ($v_{O^+} = v_{H^+} = 0$ at the equator crossing of field line), then (6) and (7) can be integrated to give the transport velocities

$$v_{O^+} = \frac{B}{[O^+]} \int_s^{s_e} \left(\partial [O^+]/\partial t - p[O] + L[O^+]\ [N_2] + 9/8K[O^+]\ [H] - K[O]\ [H^+]\right) ds/B \tag{8}$$

$$v_{H^+} = \frac{B}{[H^+]} \int_s^{s_e} \left(\partial [H^+]/\partial t - 9/8K[O^+]\ [H] + K[O]\ [H^+]\right) ds/B \tag{9}$$

where s_e is the distance up the field line to the equator.

The Momentum Equations

Defining the ion and electron scale heights H_{H^+}, H_{O^+}, H_e as,

$$\begin{aligned} 1/[H^+]\ \partial [H^+]/\partial s &= -1/H_{H^+} \\ 1/[O^+]\ \partial [O^+]/\partial s &= -1/H_{O^+} \\ 1/N_e\ \partial N_e/\partial s &= -1/H_e\ , \end{aligned} \tag{10}$$

the equations of momentum conservation can be written in the form

$$\frac{1}{H_{O^+}} + \frac{T_e}{T_i}\frac{1}{H_e} = \frac{1}{T_i}\frac{\partial (T_e + T_i)}{\partial s} + \frac{m_{O^+} g}{kT_i} + \frac{\theta_{O^+H^+}\ [H^+]}{kT_i}\left(v_{O^+} - v_{H^+}\right) + \frac{\theta_{O^+O}\ [O]}{kT_i}\left(v_{O^+} - v_O\right) \tag{11}$$

$$\frac{1}{H_{H^+}} + \frac{T_e}{T_i}\frac{1}{H_e} = \frac{1}{T_i}\frac{\partial(T_e + T_i)}{\partial s} + \frac{m_{H^+} g}{kT_i} + \frac{\theta_{O^+H^+}[O^+]}{kT_i}\left(v_{H^+} - v_{O^+}\right) + \frac{\theta_{H^+H}[H]}{kT_i}\left(v_{H^+} - v_H\right) \quad (12)$$

where

g = acceleration parallel to the field due to gravity

m_{O^+}, m_{H^+} = ion masses

k = Boltzmann's constant

T_e, T_i = electron and ion temperatures

θ_{xy} = drag coefficients for collisions between species x and y.

The ion-ion and ion-neutral drag terms on the right of Equations (11) and (12) are zero in diffusive equilibrium because there is by definition no relative motion between the various ion and neutral species. If a dynamic condition exists, however, the drag terms will be non-zero and will either increase or decrease the ion and electron scaleheights from their diffusive equilibrium values. A downward drag on the ions aids the gravitational force and decreases the ion scale heights. Conversely, if the drag forces are upward, the ion scale heights increase. The former is needed to explain the reduced scale height of O^+ below 500 kilometers observed on this flight.

Sources of Ion-Neutral Drag

For O^+, ion-ion drag between O^+ and H^+ can be neglected below 500 kilometers because the concentration of protons is small at these altitudes. Ion-neutral

drag at these altitudes can be large however since the neutral concentrations are large.

If we assume that motions in the neutral atmosphere were responsible for the reduced scale height, we require a 25 meter/sec component of the neutral wind down the field line. King and Kohl (1965) and Geisler (1966) showed that the global pressure distribution can produce poleward winds on the dayside of the Earth which are of the right order.

If on the otherhand we invoke an upward flux of O^+ induced by a temporal variation in O^+, an upward ion velocity of 15 meters/second also could account for the reduced scale height observed at 300 kilometers. Fluxes of this order might be expected from the normal diurnal variation of the ion distribution.

Theoretical Fit to the Data

In this section we describe a simultaneous solution to the particle, momentum and energy equations which fits the composition, density and temperature measurements. We solved the O^+ and H^+ continuity and momentum equations by adopting the measured N_e as a boundary condition at the base altitude of 300 kilometers. The H^+ concentration is assumed to be in chemical equilibrium below 400 kilometers (as demonstrated by Brinton et al., 1968), a factor which provided the necessary additional boundary condition for deriving the ion composition. For the neutral composition and temperature, the low solar activity model of Jacchia (1964) was employed, except that the higher concentration of hydrogen derived by Brinton, et al., (1968) was used ($[H] = 5 \times 10^5$ cm^{-3} at 300 kilometers).

The electron and ion temperatures employed in the momentum equations were derived simultaneously from the energy equations employed by Mayr, Brace and Crevier (1968). The energy input rates for local and non-local heating were adjusted to closely reproduce the T_e observations above 300 kilometers as shown in Figure 7. The calculated T_i and the neutral temperature are also shown. A local heating rate of 4.5×10^{-6} [O] eV cm^{-3} sec^{-1} and a fast electron flux of 6×10^8 cm^{-2} sec^{-1} of 10 eV electrons provided the best fit.

Finally, we adjusted the upward O^+ flux $\left(v_{O^+}\right)$, or conversely the downward O flux $\left(v_O\right)$, to fit the entire N_e profile between 300 and 600 kilometers.

Figure 8 compares the measured downleg N_e profile (corrected slightly near apogee for the horizontal gradient of N_e) with the theoretical profile resulting from either an upward O^+ flux of 5.5×10^8 cm^{-2} sec^{-1} or a down-the-field component of the neutral wind of 25 meters per second. A diffusive equilibrium profile employing the same temperatures is also shown for comparison.

Although either the upward ion flux or the downward neutral wind component could equally well be used to fit the measurements, Brinton et al. have concluded that their measurements of N^+ ions on this flight are inconsistent with an upward flux of O^+. Their N^+ results are, however, consistent with the neutral wind we have invoked to explain the N_e scale height.

CONCLUSIONS

We have concluded that diffusive equilibrium did not exist in the upper F region at the time of this flight because of dynamic effects in either the neutral

atmosphere or in the ionosphere. The rocket measurements of T_e and N_e were reproduced by introducing either (1) a neutral wind which has a downward component of 25 meters per second along the magnetic field or (2) an upward ion flux of 6×10^8 cm^{-2} sec^{-1} produced by a temporal variation in N_e.

ACKNOWLEDGMENTS

We are grateful to G. R. Carignan of the University of Michigan for development and fabrication of the electronics employed in this experiment and to Milton Sing of Goddard Space Flight Center for his aid in the analysis of the data.

REFERENCES

Brace, L. H., B. M. Reddy, "Early electrostatic probe results from Explorer 22," J. Geophys. Res., 70, 5783, 1965.

Brace, L. H., B. M. Reddy, H. G. Mayr, "Global behavior of the ionosphere at 1000 kilometer altitude," J. Geophys. Res., 72, 265, 1967.

Brinton, H. C., M. W. Pharo, III, H. G. Mayr, H. A. Taylor, Jr., "A direct measurement of ion composition in the daytime F_2-Region; implications for ionospheric chemistry and dynamics," (submitted to J. Geophys. Res.), 1968.

Cooley, J. E., C. A. Reber, "Neutral composition measurements between altitudes of 140-480 kilometers made by the Geoprobe Mass Spectrometer," J. Geophys. Res., (submitted).

Geisler, J. E., "Atmospheric winds in the middle latitude F-region," J. Atmospheric Terr. Phys., 28, 703, 1966.

Jacchia, L. G., "The temperature above the thermopause," Smithsonian Astrophys. Observ., Rept. 150, April 22, 1964.

King, J. W., H. Kohl, "Upper atmospheric winds and ionospheric drifts caused by neutral air pressure gradients," Nature, 206, 609, 1965.

Mayr, H. G., L. H. Brace, W. Crevier, "The latitudinal temperature structure of the topside ionosphere," (submitted to J. Geophys. Res.)

Pelz, D. T., G. P. Newton, "Midlatitude neutral thermosphere density and temperature measurements," J. Geophys. Res., 73, 1968.

Spencer, N. W., L. H. Brace, G. R. Carignan, D. R. Taeusch, H. Niemann, "Electron and molecular nitrogen temperature and density in the thermosphere," J. Geophys. Res., 70, 2665, 1965.

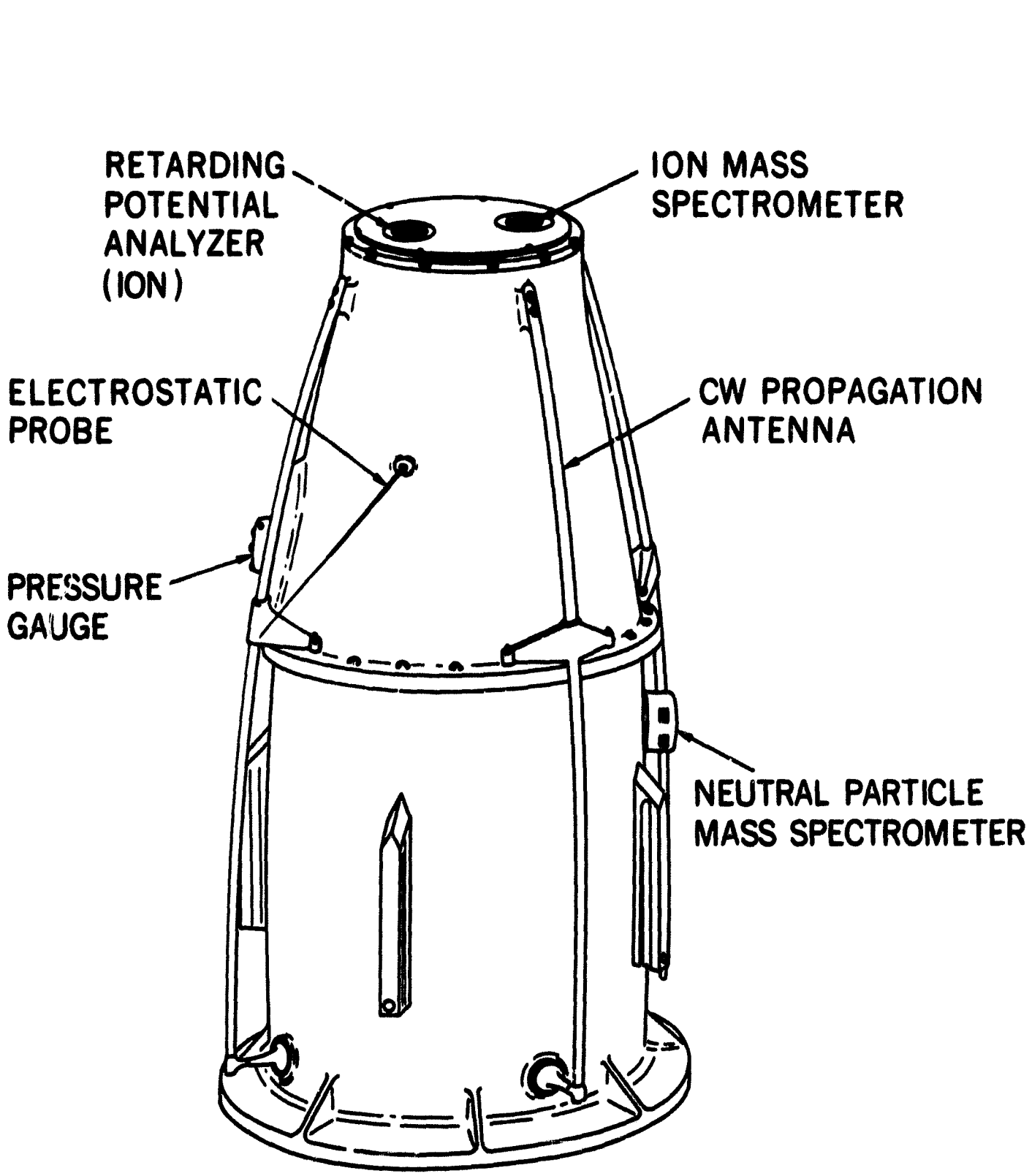

Figure 1. Drawing of NASA 8.25 payload showing electrostatic probe mounted perpendicular to the spin axis. The other experiments, not discussed in this paper, are also shown.

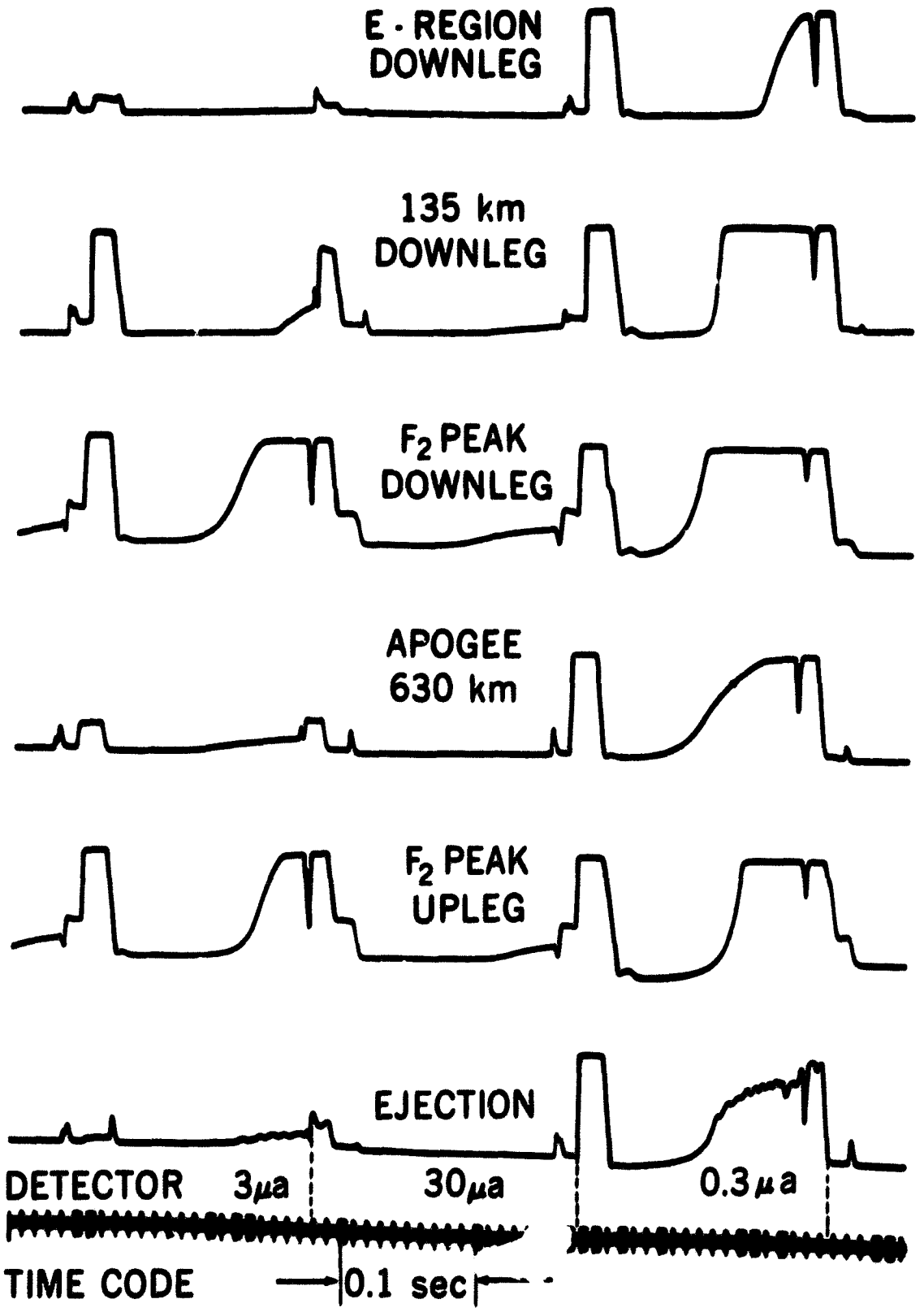

Figure 2. Photograph of sections of telemetry record arranged vertically to show typical characteristics obtained on the three current ranges at selected intervals through the flight. Reading upward, the curves taken immediately after ejection of the nose cone show fine structure and are depressed in amplitude. Later curves at the F_2 peak, apogee, the F_2 peak and in the E region are smooth. The plateaus before and after each curve represent the electron saturation currents at +5 volts applied potential.

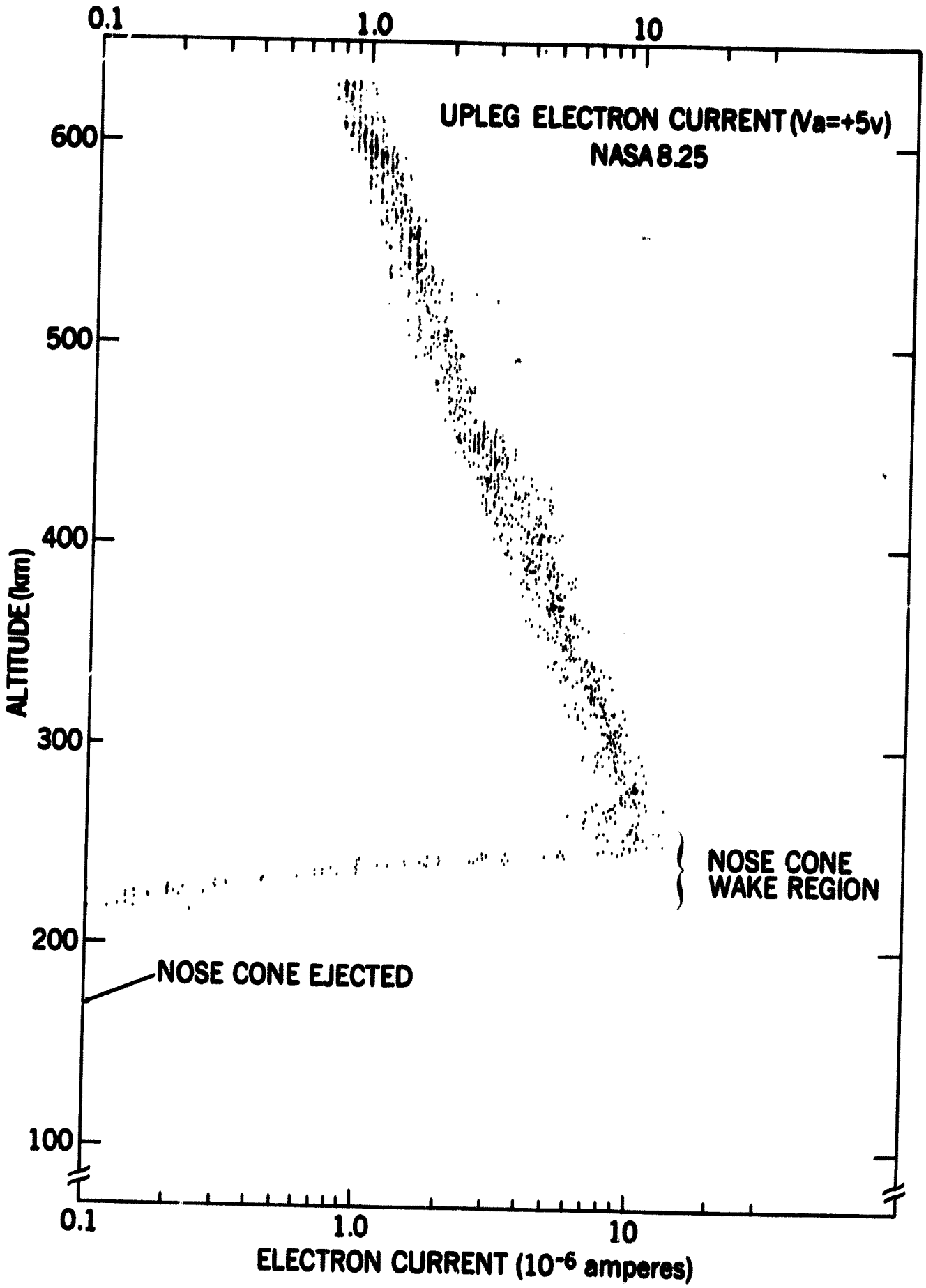

Figure 3. Electron currents (at +5 volts) measured on upleg of NASA 8.25, 17:59:42 UT, March 2, 1966 at Wallops Island, Va. The nose cone wake effects were strong below 260 kilometers.

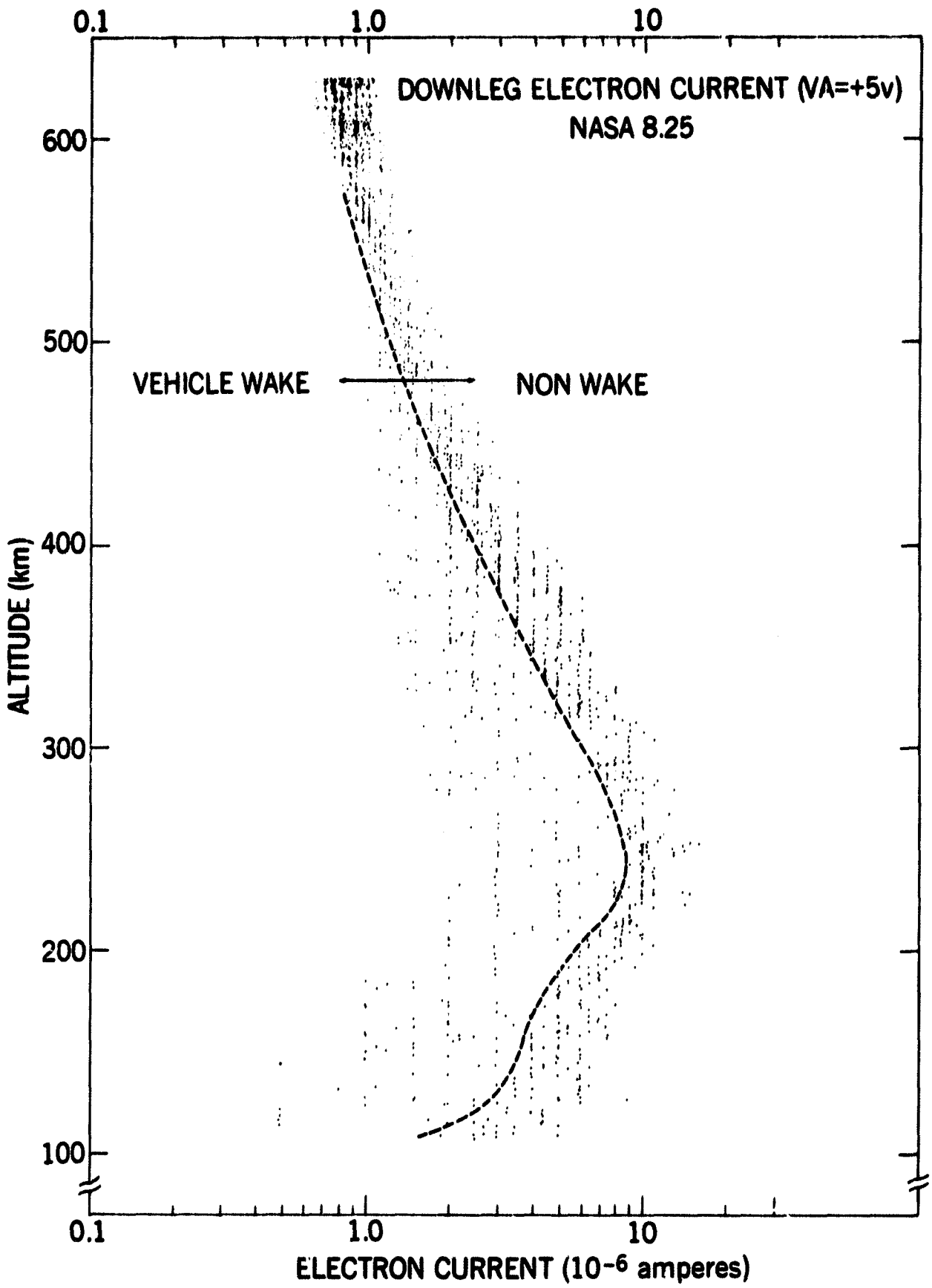

Figure 4. Electron currents on downleg of NASA 8.25. The wide scatter at lower altitudes results from the passage of the probe through the vehicle's wake as the payload spins. The currents below the dashed line were rejected for this reason.

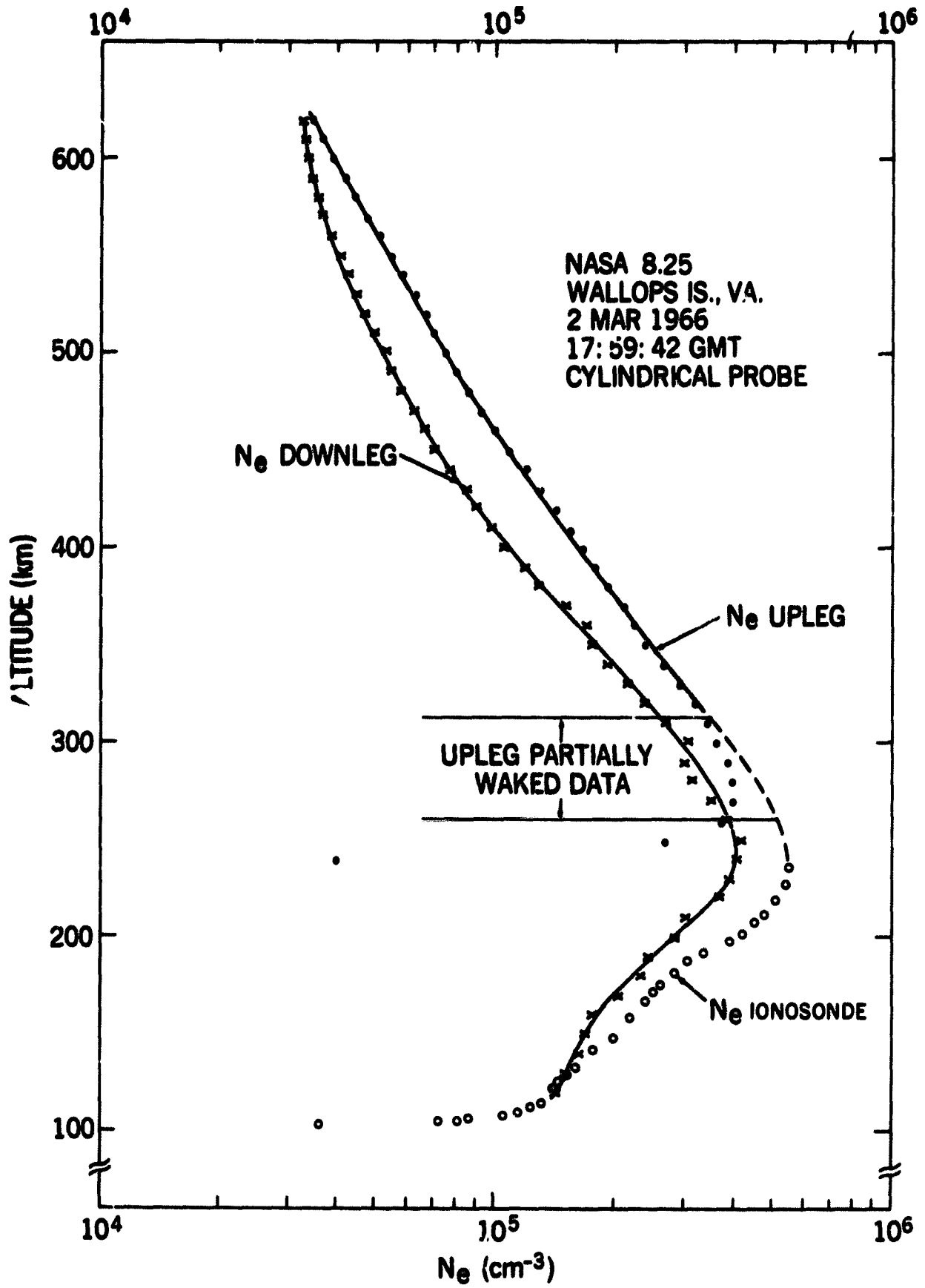

Figure 5. N_e measurements on an altitude scale. The dashed line is interpolated between the ionosonde measurements and the non-wake probe measurements above 320 kilometers. The horizontal gradient, which is evident from the upleg-downleg difference, may have significantly distorted the profiles above about 500 km.

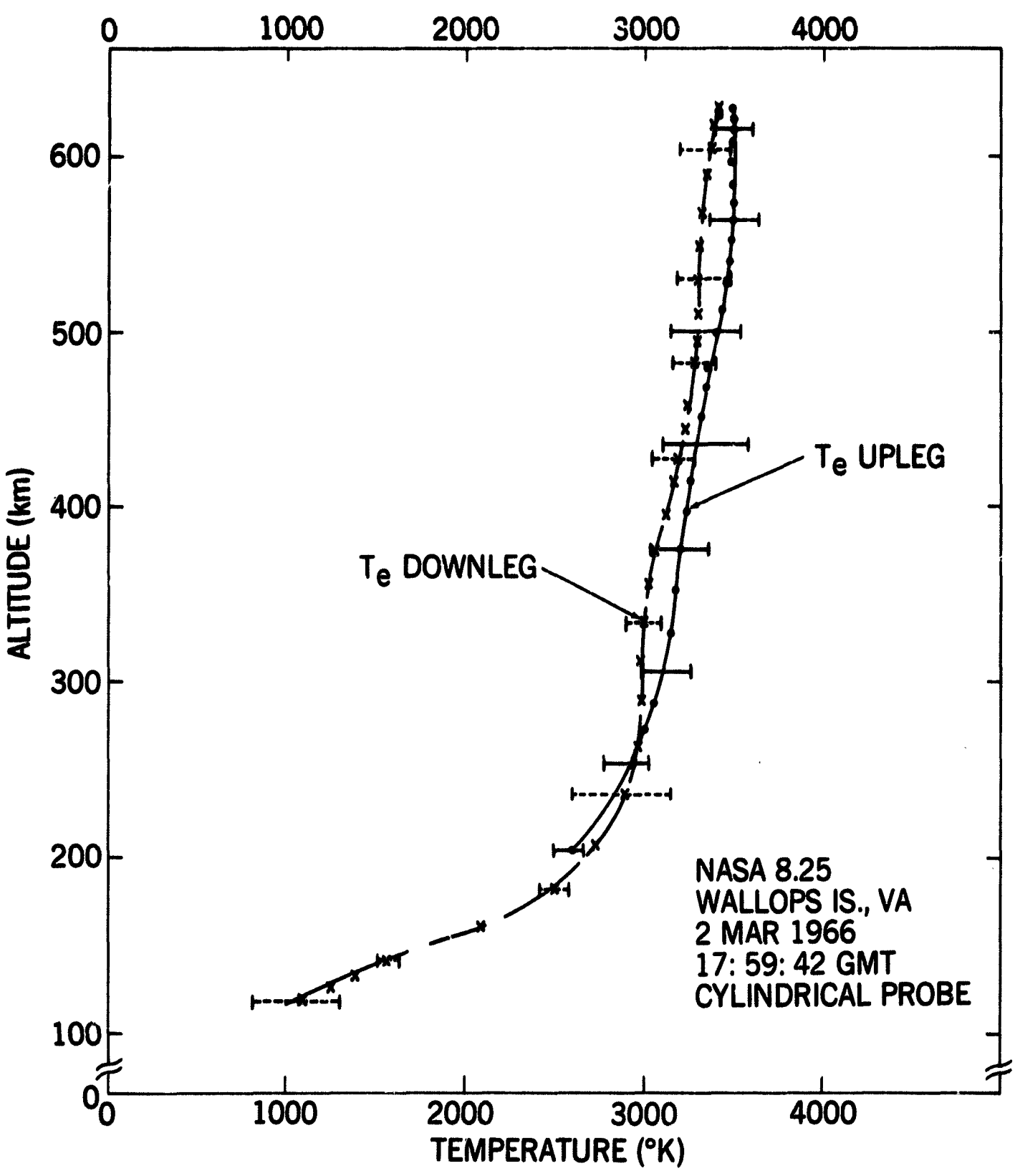

Figure 6. The T_e measurements. The points represent the mean of the temperatures from about 5 consecutive curves taken over less than a 5 kilometer interval. Groups of curves selected for analysis were spaced at about 20 kilometer intervals. The horizontal bars representing the standard deviation of the set are considered typical.

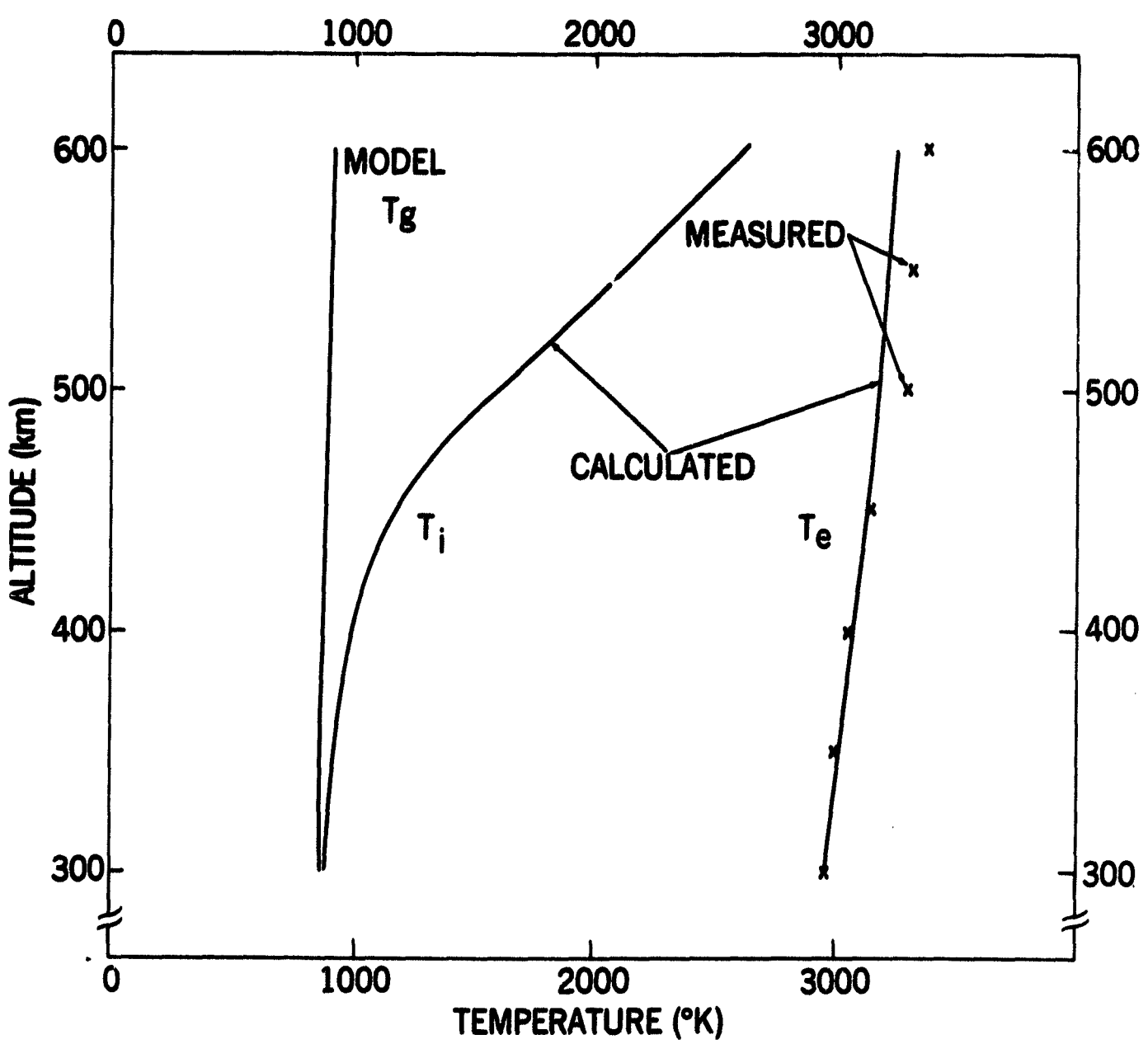

Figure 7. Comparison between calculated and measured T_e. The model T_g and calculated T_i profiles are shown.

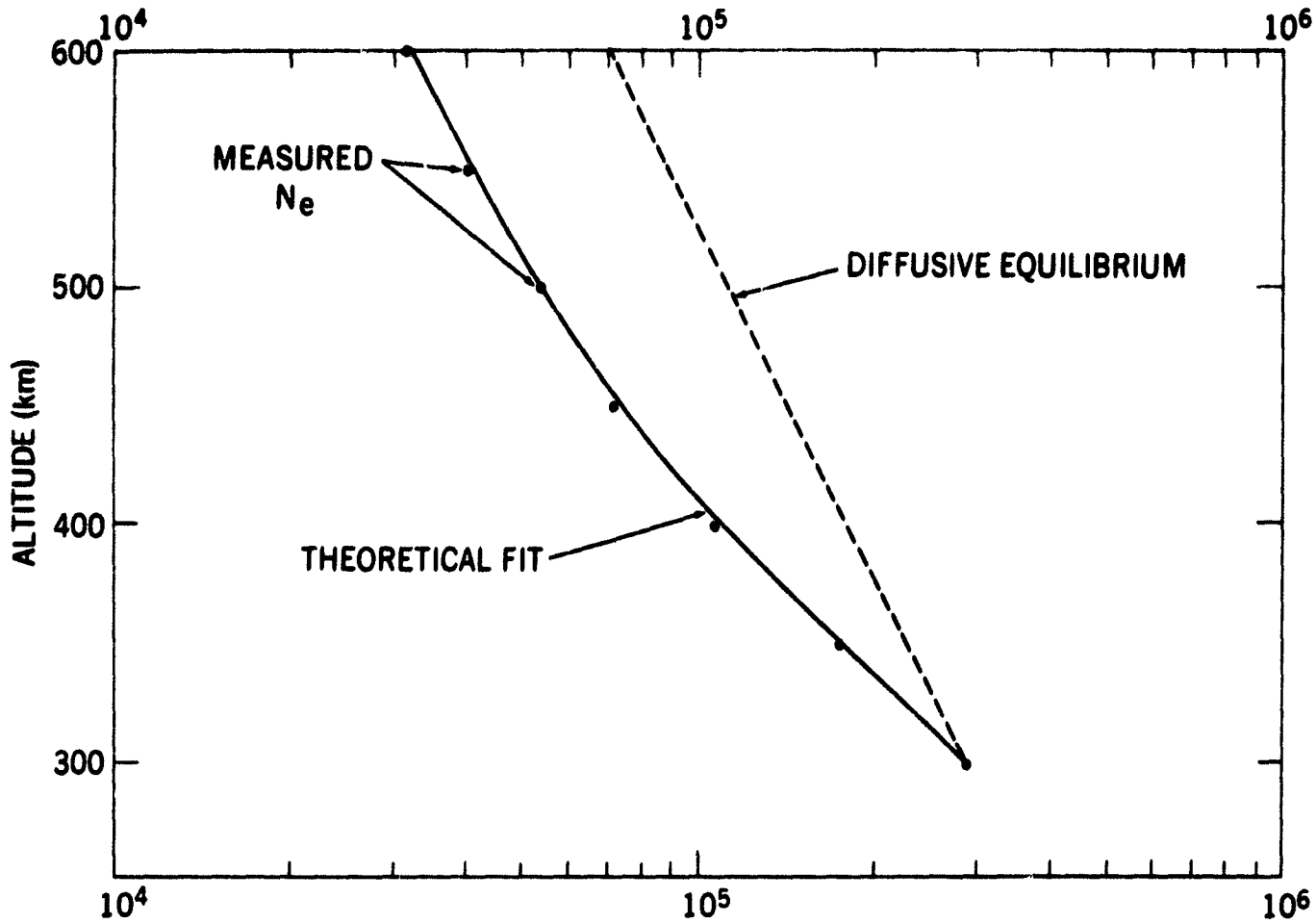

Figure 8. Theoretical fit to the measured N_e profile employing downward wind component of 25 meters/sec. An equally good fit is obtained by assuming an upward O^+ flux of 5.5×10^8 cm^{-2} sec^{-1}. The corresponding diffusive equilibrium profile has a much greater scale height below 450 kilometers.